Published in final edited form as:

Mol Cancer Ther. 2017 February ; 16(2): 344–356. doi:10.1158/1535-7163.MCT-16-0337.

Dual Inhibition of MEK and PI3K/Akt Rescues Cancer Cachexia through Both Tumor Extrinsic and Intrinsic Activities

Erin E. Talbert[#a,b], **Jennifer Yang**[#a,c], **Thomas A. Mace**[a,d], **Matthew R. Farren**[a,d], **Alton B. Farris**[e], **Gregory S. Young**[f], **Omar Elnaggar**[d], **Zheng Che**[d], **Cynthia D. Timmers**[a], **Priyani Rajasekera**[a], **Jennifer M. Maskarinec**[g], **Mark Bloomston**[a,h,3], **Tanios Bekaii-Saab**[a,4], **Denis C. Guttridge**[a,b,c,2], and **Gregory B. Lesinski**[a,d,2,5]

[a]Arthur G. James Comprehensive Cancer Center Cancer Cachexia Program, The Ohio State University Medical Center, Columbus, Ohio 43210, USA

[b]Department of Molecular Virology, Immunology, and Medical Genetics, The Ohio State University Medical Center, Columbus, Ohio 43210, USA

[c]Molecular, Cellular, and Developmental Biology Program, The Ohio State University Medical Center, Columbus, Ohio 43210, USA

[d]Department of Internal Medicine, Division of Medical Oncology, The Ohio State University Medical Center, Columbus, Ohio 43210, USA

[f]Center for Biostatistics, The Ohio State University Medical Center, Columbus, Ohio 43210, USA

[g]Biomedical Science Program, The Ohio State University Medical Center, Columbus, Ohio 43210, USA

[h]Division of Surgical Oncology, The Ohio State University Medical Center, Columbus, Ohio 43210, USA

[e]Pathology & Laboratory Medicine, Emory University School of Medicine, Atlanta, Georgia 30307, USA

[#] These authors contributed equally to this work.

Abstract

Involuntary weight loss, a part of the cachexia syndrome, is a debilitating co-morbidity of cancer and currently has no treatment options. Results from a recent clinical trial at our institution showed that biliary tract cancer patients treated with a MEK inhibitor exhibited poor tumor responses, but surprisingly gained weight and increased their skeletal muscle mass. This implied that MEK inhibition might be anti-cachectic. To test this potential effect of MEK inhibition, we utilized the established Colon-26 model of cancer cachexia and the MEK1/2 inhibitor MEK162. Results

[2]**Address for Correspondence:** Gregory B. Lesinski, Department of Hematology and Medical Oncology, Winship Cancer Institute of Emory University, 1365 Clifton Rd. NE, Atlanta, GA, 30322. Tel: (404)-778-5419; gregory.b.lesinski@emory.edu, and Denis C. Guttridge, 520 Biomedical Research Tower, 460 W 12th Avenue, Columbus 43210 OH, USA; Phone: (+1) 614-688-3137; Fax: (+1) 614-292-6356; denis.guttridge@osumc.edu.

[3]Current address: South Florida Surgical Oncology, 4571 Colonial Blvd. Suite 100 Fort Myers, FL 33966

[4]Current address: Mayo Clinic, 5777 E. Mayo Blvd, Phoenix, AZ, 85054

[5]Current address: Winship Cancer Institute of Emory University, 1365 Clifton Rd. NE, Atlanta, GA, 30322

Conflict of Interest: None of the authors in this study declare a conflict of interest.

showed that MEK inhibition effectively prevented muscle wasting. Importantly, MEK162 retained its ability to spare muscle loss even in mice bearing a Colon-26 clone resistant to the MEK inhibitor, demonstrating that the effects of blocking MEK is at least in part independent of the tumor. Because single agent MEK inhibitors have been limited as a front-line targeted therapy due to compensatory activation of other oncogenic signaling pathways, we combined MEK162 with the PI3K/Akt inhibitor buparlisib. Results showed that this combinatorial treatment significantly reduced tumor growth due to a direct activity on Colon-26 tumor cells *in vitro* and *in vivo*, while also preserving skeletal muscle mass. Together, our results suggest that as a monotherapy MEK inhibition preserves muscle mass, but when combined with a PI3K/Akt inhibitor exhibits potent anti-tumor activity. Thus, combinatorial therapy might serve as a new approach for the treatment of cancer cachexia.

Keywords

cancer cachexia; muscle wasting; muscle atrophy

Introduction

The Ras/Raf/MEK/ERK pathway, which promotes cell growth and survival, is mutated in nearly 40% of all human tumors. Although inhibition of Ras is an attractive therapeutic strategy, designing specific anti-Ras compounds has been elusive (1). Thus, efforts have shifted to targeting the downstream effectors of Ras, MEK and ERK. In addition to regulating tumor cell proliferation and survival, the Ras/Raf/MEK/ERK pathway is also known to promote the production of cytokines from malignant cells (2-5). The aberrant production of soluble factors is thought to contribute to systemic changes that are prominent in patients with advanced cancer, including the cancer cachexia syndrome (6). Cancer cachexia is characterized by the loss of skeletal muscle and adipose tissue mass, which cannot be reversed by nutritional intervention (7). More than half of all cancer patients experience cachexia, and cachexia is a significant contributor to mortality from cancer (8, 9). Currently, no effective pharmacologic approach exists to limit cancer cachexia.

Recently, a particularly interesting observation was made in a clinical trial with biliary tract cancer patients treated with the MEK inhibitor selumetinib. In this trial, only 12% of patients had objective responses to therapy, but 80% of the patients treated with MEK inhibition experienced significant weight gain associated with increases in skeletal muscle mass (10, 11). Since weight gain is unusual in biliary tract cancer patients given their high incidence of cachexia, these clinical data suggested that MEK inhibition might possess an anti-cachectic activity.

To investigate the potential that MEK inhibition might serve as an anti-cachexia therapy, we initiated a pre-clinical study using the MEK inhibitor MEK162 in an established mouse model of cancer cachexia, the Colon-26 (C-26) tumor model (12, 13). Similar to prior clinical observations in biliary tract cancer patients, results showed that MEK162 preserves skeletal muscle mass. Although effective at maintaining skeletal muscle, we recognize that ultimately, future successful anti-cancer therapy will need to maximize the protection of host

tissues while targeting malignant cells. Because resistance to MEK inhibition is often associated with a compensatory activity on the PI3K/Akt pathway (14), we treated C-26 tumor-bearing mice with a combination of MEK162 and the PI3K/Akt inhibitor, buparlisib. Results showed that this combination led to a potent inhibition of both tumor growth and cachexia, resulting from a direct cytotoxic activity on C-26 tumor cells. Together, these results successfully uncouple multiple mechanisms by which MEK inhibition may benefit patients with advanced cancer, including a tumor extrinsic effect that preserves skeletal muscle and a tumor intrinsic activity that reduces tumor load due to the improved efficacy of PI3K/Akt inhibition.

Materials and Methods

Initial Study Design

Male CD2F1 mice seven to eight weeks of age were purchased from Charles River Laboratories (Wilmington, MA), randomly assigned to treatment groups, housed in conventional conditions, and fed a standard ad libitum rodent chow diet at University Laboratory Animal Services at the Arthur G. James Comprehensive Cancer Center of The Ohio State University. Colon-26 (C-26) adenocarcinoma cells were maintained in RMPI-1640 media containing 5% fetal bovine serum. Mice were randomized between treatment groups and then injected subcutaneously in the right flank with 1×10^6 murine C-26 cells. Animals were monitored daily, with body weight and bi-dimensional tumor measurements obtained three times weekly using microcalipers. Experiments were terminated when the body condition score of mice in the vehicle treatment group decreased to 1.5 or lower (15), which is consistent with recommendations made by the laboratory animal veterinary staff at The Ohio State University. In the C-26 model, this body condition score is associated with an approximately 20% weight loss. Mice with ulcerated tumors were removed from the study prior to the final endpoint and were excluded from all data analysis. No outliers were excluded from the data analysis. Similar procedures were followed for experiments using Lewis Lung Carcinoma (LLC) tumors, with the following modifications: (1) LLC tumor cells were maintained in Dulbecco's Modified Eagle's Media containing 5% fetal bovine serum and (2) 5×10^5 tumor cells were injected into the right gluteus muscles of C57B/6 mice purchased from Jackson Labs (Bar Harbor, ME). Both our C-26 and LLC cell lines were obtained through a Material Transfer Agreement with the National Cancer Institute in 2001. These cell lines have been maintained in the Guttridge Laboratory and have consistently produced similar cachexia, including in this manuscript, demonstrating that these cells have maintained their identity over time (12, 16). All animal experiments were approved by the Institutional Animal Care and Use Committee of The Ohio State University under protocol 2010A00000177-R1 in accordance with the NIH Guide for Care and Use of Laboratory Animals. *In vitro* experiments were performed a minimum of three times to ensure veracity of the data.

Drug Treatment

MEK162 and buparlisib were provided by Novartis, Inc. (Basel, Switzerland) as lyophilized stocks and resuspended in DMSO to a concentration of 100mM for *in vitro* experiments. For *in vivo* experiments, the inhibitors were resuspended at a concentration of 100 μg/mL in 1%

carboxymethyl cellulose and 0.5% Tween 80, with MEK162 given at a dose of 30 mg/kg and buparlisib given at 25 mg/kg. These dosages are consistent with previous clinical trials (17, 18). Vehicle-treated animals received 1% carboxymethyl cellulose, 0.5% Tween 80. All treatments were administered via oral gavage in a volume of 200 μL daily. Chemical structures of the inhibitors are available in (19) and (20).

MEK162-Resistant C-26 Cells

To generate a line of tumor cells resistant to MEK162, C-26 cells were seeded in 6-well plates at 1×10^6 cells/well overnight. Cells were then treated with MEK162 beginning at 1μM for 3 days and increased to 30 μM incrementally over a 2-week period. MEK162 concentration was increased when cell confluence increased. Resistance of C-26 cells to MEK162 was validated using an MTT assay. The subsequent MEK162 resistant C-26 cell line was designated 'C-26R'. Prior to implantation *in vivo* for therapeutic studies, C-26R cells were maintained in the presence of MEK162 (30 μM) to ensure maintenance of MEK162 resistance. Similar to our parental line studies, 1×10^6 C-26R cells were injected into the right flank of randomized groups of mice. For our *in vivo* C-26R studies, our animal initial numbers were based upon our findings in our first experiments utilizing our parental line. However, due to the aggressive nature of our resistant tumor cells, we repeated these experiments to ensure that our findings were accurate. After achieving the same results, we collapsed our two data sets.

Muscle Cross-sectional Area

Muscle cross-sectional area was determined in the gastrocnemius muscle. Ten μm sections were cut from muscles frozen in liquid nitrogen-cooled isopentane. Three sections representing the entire length of the muscle were selected for H&E staining and images were acquired using an Olympus BX51 bright field microscope. The Olympus Microsuite Pathology software was used to determine individual muscle fiber CSA by manual outlining with software assistance. Results from all three sections from each animal were averaged prior to statistical analysis. Across all experiments, an average of 316 fibers per section and 930 total fibers per animal were analyzed.

Real-time Reverse Transcriptase PCR

Messenger RNA was isolated from snap-frozen quadriceps muscle using Trizol reagent (Life Technologies, Carlsbad, CA) according to the manufacturer's instructions. Total RNA was reverse-transcribed to cDNA using M-MLV Reverse Transcriptase (Life Technologies) according to the manufacturer's instructions. Real-time PCR was performed on an Applied Biosystems StepOnePlus instrument using SYBR Green mix (Bio-Rad, Hercules, CA). GAPDH was used as the housekeeping gene. Primer sequences appear in Supplementary Table 1.

Tumor Immunohistochemistry

Following euthanasia, tumors were removed and formalin-fixed overnight before undergoing processing and paraffin embedding. For our initial experiments with the parental tumor cells, tumors were sectioned at 4 μm. Slides were deparaffined, rehydrated, then stained with anti-

phospho-p42/p44 (phospho-ERK, Cell Signaling Technology (CST) #4370) using the Dako Autostainer Immunostaining System, with Vulcan Fast Red™ or BiocareRomulin AEC chromogens and counterstained with Richard Allen hematoxylin. Tumors were analyzed in a blinded fashion by a board-certified pathologist (Dr. Alton Brad Farris, Emory University). For all additional experiments, tumors were sectioned at 5 μm and stained using a Bond Rx autostainer (Leica). Slides were heated for 15 minutes at 65°C and then automated software dewaxed, rehydrated, performed antigen retrieval, blocked, incubated with primary antibody, detected (DAB), and counterstained using Bond reagents (Leica). Samples were then removed from the machine, dehydrated through ethanols and xylenes, mounted and coverslipped. The following antibodies were diluted in Leica antibody diluent: anti-phospho-pERK (Thr202/Tyr204) (Cell Signaling Technology (CST) #4370), anti-pAKT (Thr308, CST #9275), CD3 (Dako A0452), cleaved caspase-3 (CST #9661), or Ki67 (Abcam ab16667). Quantification of cells positive for CD3, cleaved caspase-3, and Ki67 was performed using the Vectra Automated Quantitative Pathology Imaging System and the InForm Software (PerkinElmer).

Immunoblot Analysis

Immunoblots on tumor cells were performed as previously described and probed with antibodies specific for pERK (Thr202/Tyr204, CST #4370), ERK (CST #4695), pAKT (Thr308, CST #9275), AKT (CST #9272) (21). Western blotting on muscle tissues was conducted as previously described using pERK (Thr202/Tyr204, CST #4370) or LC3B (CST #2775), fluorescently conjugated secondary antibodies, and a Li-Cor Odyssey imaging system (13). β-actin (CST #4967) or α-tubulin (Sigma T5168) were used as loading controls.

Phenotypic Analysis of Splenocytes by Flow Cytometry

Phenotypic analysis of the myeloid derived suppressor cell (MDSC) and T lymphocyte populations in splenocytes from mice was conducted using standard methods. Briefly, 10^6 splenocytes were resuspended in 100 μL of FACS buffer (PBS+5% FBS) and incubated with fluorochrome-labeled antibody targeting murine CD11b (BD Biosciences #557686), GR1 (BD #553127), CD4 (BD #552775), CD8 (BD #552877), or appropriate isotype control antibody (BD Biosciences) for 1hr at 4°C. Cells were washed, resuspended in 1% formalin and analyzed via flow cytometric analysis on a LSRII flow cytometer (BD Biosciences).

$CD4^+$ and $CD8^+$ T Cell Depletion

Antibody depletion of $CD4^+$ and $CD8^+$ cells were conducted as previously described (22). Briefly, rat anti-mouse CD8 (clone 2.43) and rat anti-mouse CD4 (clone GK1.5) antibodies were purchased from Bio X Cell (West Lebanon, NH). For depletion experiments, 100 μg of antibody was injected intraperitoneally on days −3, −1, +1, +3 and every 4 days thereafter in relation to the tumor injection (on Day 0). Purified Rat IgG was used as a control (Sigma, St. Louis, MO). Depletion of $CD4^+$ and $CD8^+$ cells was confirmed by flow cytometric analysis of lymphocytes obtained from splenocytes at the study endpoint.

Cellular Growth Assay

C26 cell lines were seeded in 96-well plates in triplicate and allowed to adhere overnight. Fresh media containing MEK162, buparlisib, or both was added to each well at various concentrations (5 and 10 μM of MEK162, and 2.5 and 5 μM of buparlisib) and cells were incubated for 72 hours. At this time, the percentage of cell growth was evaluated using the MTT assay (ATCC 30-1010K) and quantified by determining the optical density at 595 nm using a Bio-Rad iMark™ microplate reader.

Statistics

All data are displayed as mean ± SEM. For experiments comparing MEK162 treatment to vehicle treatment, differences between group means were determined using a two-tailed Student's *t*-test. Experiments assessing treatment with MEK162, buparlisib, and MEK162 + buparlisib in combination were analyzed utilizing one-way ANOVA with Tukey's HSD post hoc when appropriate, with the exception of tumor growth and weight. The rate of tumor growth was determined using a mixed-effects regression model on log-transformed volumes (exponential growth model). Random effects for intercept and slope by mouse were included and slopes were compared using linear contrasts. Body weights were analyzed using a linear model with fixed effects for group, time and the group by time interaction. A first-order autoregressive covariance structure for the residual error was used and p-values were adjusted using the Bonferroni method. Degrees of freedom were determined by the Kenward-Roger method (23). Log transformations were used when appropriate to eliminate the effects of heteroscedasticity and are noted in the figure legends of transformed data. All analyses were performed in SAS v9.4 (SAS Institute, Cary, NC). P values less than 0.05 were considered significant.

Results

MEK inhibition prevents muscle wasting in tumor bearing mice

Biliary cancer patients display a high incidence of cachexia, but patients treated with MEK inhibition regained body weight in the form of lean mass (10, 11). This suggested that MEK might be a therapeutic target in cancer cachexia. To examine the impact of MEK inhibition on cachexia, we utilized the established Colon-26 (C-26) cancer cachexia model. CD2F1 mice bearing palpable C-26 tumors were dosed with a MEK1/2 specific inhibitor, MEK162. Daily treatment for 16 days with MEK162 had a pronounced effect at preventing tumor-induced body weight loss as compared to vehicle-treated animals (Fig. 1A). To assess whether this activity of MEK162 was derived from the protection of lean mass, hindlimb muscles from tumor-bearing mice were analyzed. Results showed that MEK162-treated mice had larger tibialis anterior (TA), quadriceps (QUAD), and gastrocnemius (GAST) muscle masses compared to vehicle controls (Fig. 1B). In addition, the increase in muscle weight was concomitant with an increase in GAST muscle fiber size (Fig. 1C and 1D and Supplementary Fig. 1A). Furthermore, MEK162 treatment reduced the expression of a panel of established muscle atrophy genes in QUAD, including E3 ligases of the ubiquitin proteasome system (*MuRF1*, *Atrogin-1*, and *Musa1*) and genes associated with autophagy (*Atg5* and *Bnip3*) (Fig. 1E). Similar protection against muscle atrophy was seen in a second established cancer cachexia model, the Lewis Lung Carcinoma (LLC) model. LLC tumor-

bearing mice treated with MEK162 had significantly larger GAST muscle fiber cross-sectional areas compared to vehicle-treated tumor-bearing mice (Supplementary Fig. 1B, 1C, and 1D).

Significantly, when non-tumor-bearing CD2F1 mice were treated with a similar dosing regimen of MEK162, total body weight and muscle mass remained unchanged, demonstrating that MEK162 does not function simply as an anabolic agent to increase skeletal muscle mass (Supplementary Fig. 1E and 1F). These data, coupled with our previous work demonstrating that our C-26 tumor-bearing mice do not exhibit decreased food intake compared to mice without tumors (24), suggest that a mechanism other than increased food intake is responsible for the anti-cachexia effect of MEK162. Comparison of muscle weights from C-26 tumor-bearing mice to non-tumor-bearing controls demonstrate that MEK162 provides a nearly complete rescue of muscle mass for all three of the muscles tested (Supplementary Fig. 1G).

MEK inhibition limits muscle wasting in the C-26 model in part through a tumor extrinsic effect

A common problem plaguing cancer cachexia research is that while many compounds appear to be anti-cachectic, their ability to rescue muscle wasting actually results from a direct effect on tumors and not a protection of host tissues (25-27). As such, any treatment that is effective at reducing the tumor load would be expected to have a downstream benefit of rescuing muscle wasting. When we examined changes in tumor volume in our mice treated with MEK162, we found that MEK inhibition exhibited a modest effect on the rate of C-26 tumor growth, although this was not statistically significant (Fig. 2A). Nevertheless, MEK162 treatment reduced ERK activity in C-26 tumors (Fig. 2B), demonstrating its on-target activity. Further, MEK162 significantly reduced serum levels of IL-6 (Supplementary Fig. 2A), which in this model has been shown to be tumor-derived and functions as a major driver of cachexia (28-30). These data suggested that the anti-cachectic activity of MEK162 is associated with some effects on the tumor. However, upon examining ERK activity within skeletal muscle, we also observed that MEK162 treatment was effective in reducing tumor-induced increases in ERK phosphorylation (Supplementary Fig. 2B), implying that a portion of the anti-cachectic effect of inhibiting MEK could be tumor extrinsic.

In an attempt to determine whether the anti-cachectic activity of MEK inhibition could be uncoupled from its tumor effect, we set out to produce a C-26 tumor line that was resistant to MEK162. To produce this line, we continually cultured C-26 tumor cells in increasing concentrations of MEK162 until tumor cells became resistant to its cytotoxicity, and ERK activity could no longer be inhibited (Fig. 2C and 2D). We named these resistant cells C-26R, to distinguish them from the C-26 parental line. Similar to resistance *in vitro*, the growth of implanted C-26R tumor cells in mice was nearly indistinguishable between vehicle- and MEK162-treated mice (Fig. 2E and Supplementary Fig 2C). In addition, compared to the pronounced effect that MEK162 had on reducing circulating IL-6 levels from parental C-26 tumors (Supplementary Fig. 2A), serum IL-6 from MEK162-treated C-26R tumor-bearing mice was actually higher than vehicle-treated C-26R mice

(Supplementary Fig. 2D), providing further evidence that we had established a cell line resistant to MEK162.

Several distinguishing features were observed with the C-26R cell line. In culture, the morphology of these cells appeared different than C-26 parental cells, exhibiting a greater number of cell extensions that were longer (Supplementary Fig. 2E). C-26R cells tended to have slower rates of tumor growth *in vivo* compared to C-26 cells (Fig. 2F), yet mice bearing these tumors exhibited profound cachexia, reaching our endpoint criteria three days faster than parental C-26 tumor bearing mice (Fig. 2G). Consistent with this high level of cachexia, serum IL-6 levels of vehicle-treated C-26R tumor-bearing mice were nearly five times higher than from mice bearing C-26 parental tumors (Supplementary Fig. 2A and Fig. 2D).

Importantly, despite the aggressive nature of C-26R tumors, treatment with MEK162 decreased tumor-induced body weight losses compared to vehicle-treated mice (Fig. 3A). Consistent with this preservation of body weight, C-26R tumor-bearing mice treated with MEK162 also exhibited significantly larger TA, QUAD, and GAST muscle masses compared to vehicle-treated mice (Fig. 3B). In addition, MEK162 treatment resulted in larger GAST muscle fiber size (Fig. 3C, 3D, and Supplementary Fig. 3A). Moreover, while MEK162 treatment only tended to decrease expression of proteasome genes associated with muscle atrophy, the drug significantly lowered expression of genes associated with the autophagy system in QUAD, suggesting that MEK162 decreases activation of the autophagy pathway in skeletal muscle (Fig. 3E). To confirm this finding, we probed for the autophagy-associated protein microtubule-associated protein light chain 3 (LC3). The conversion of LC3 from LC3-I to LC3-II is a commonly used surrogate marker of autophagosome formation (31). Compared to muscle from control, non-tumor-bearing mice, muscles from mice bearing C-26R tumors demonstrated increased LC3-II (Fig. 3F and 3G). In contrast, muscles from mice treated with MEK162 demonstrated reduced LC3-II conversion, suggesting that MEK inhibition reduces autophagosome formation and thus prevents atrophy by decreasing autophagic activity.

Targeting both MEK and PI3K/Akt rescues cachexia by exhibiting a strong anti-tumor activity

While MEK inhibition appears effective as an anti-cachexia treatment, ultimately, the most efficient cachexia care will require a therapy that can both limit the wasting of skeletal muscle and reduce the tumor. In many cases, tumors treated with MEK inhibition as a monotherapy develop resistance due to compensatory activation of other pro-oncogenic signaling pathways such as the PI3K/Akt pathway (14). In line with this notion, C-26 parental cells treated with MEK162 exhibited a robust activation of Akt activity (Fig. 4A). From this result, we hypothesized that treatment of C-26 tumor-bearing mice with a combination of MEK162 and an inhibitor of PI3K/Akt would be more efficacious than either drug alone. This combination of MEK162 with buparlisib is currently in clinical trials for both advanced melanoma and advanced solid tumors (NCT02159066 and NCT01363232), and thus represents a plausible clinical therapy.

The addition of the PI3K/Akt inhibitor buparlisib to MEK162 treatment had a profound effect in reducing the rate of parental C-26 tumor growth and tumor weight compared to

single agent dosing (Fig. 4B and Supplementary Fig. 4A). Staining for MEK and Akt activities in the tumors confirmed an on-target effect of MEK162 and buparlisib (Supplementary Fig. 4B).

We next asked whether this significantly improved anti-tumor response by MEK162 and buparlisib translated to an equally improved outcome on cachexia. Although buparlisib treatment alone reduced the rate of tumor growth, mice lost body weight and skeletal muscle to the same degree as vehicle-treated controls (Fig. 4C-4E, Supplementary Fig. 4C and 4D). These data are in agreement with previous reports showing that inhibition of the PI3K/Akt pathway exerts a catabolic effect on skeletal muscle (32, 33). In contrast, the combination of MEK162 and buparlisib spared body weight to a similar extent to MEK162 alone, emphasizing that MEK inhibition is dominant in protecting against cachexia (Fig. 4C and Supplementary Fig. 4C). Consistent with this notion, MEK162 and MEK162 plus buparlisib were equally efficacious in improving GAST muscle fiber cross sectional area, and reducing the expression of muscle atrophy-associated genes in QUAD compared to vehicle-treated mice (Fig. 4D-4F and Supplementary Fig. 4D). Taken together, these results revealed that while MEK inhibition alone is effective as an anti-cachexia therapy, the combination of inhibiting both MEK and PI3K/Akt signaling synergized to provide an added anti-tumor response.

MEK162 and buparlisib rescue cancer cachexia through a tumor-intrinsic activity

Next, we sought to determine what might account for the strong anti-tumor activity of combining MEK162 with buparlisib. Similar to our observations with MEK162 treatment alone, the reduction in tumor mass from MEK and PI3K/Akt inhibition associated with a decrease in circulating IL-6 (Fig. 5A). In addition to being a strong driver of cachexia in the C-26 model, IL-6 contributes to immunologic changes in advanced cancers that promote the differentiation of immunosuppressive cell populations, such as myeloid-derived suppressor cells (MDSCs), which limit T and NK cell-mediated immune function (34-36). In keeping with this function of IL-6, results showed that the percentage of splenic MDSCs, marked by cell surface markers CD11b and Gr1, declined in response to treatment with either MEK162 or buparlisib, and exhibited an even further reduction in mice treated with both compounds (Fig. 5B). We also observed that the decline in MDSCs was inversely proportional to an increase in splenic $CD4^+$ and $CD8^+$ T lymphocytes in animals treated with MEK162 and buparlisib (Fig. 5C and 5D).

Based on our findings that treatment with the combination of MEK162 was able to reconstitute the systemic adaptive immune system, we were left with two potential mechanisms by which our combination therapy was effectively reducing tumor growth. Either 1) the combinatorial therapy acted by stimulating an anti-tumor immune response, or 2) the combinatorial therapy functioned through a direct anti-tumor cell activity. To test the first of these possibilities, we depleted T cell lymphocytes using anti-CD4 and anti-CD8 antibodies in C-26 tumor-bearing mice dosed with MEK162 and buparlisib. Results revealed that removing $CD4^+$ and $CD8^+$ T lymphocytes did not abrogate the anti-tumor efficacy of MEK and PI3K/Akt inhibition (Fig. 5E, Supplementary Fig. 5A and 5B). These findings were supported by staining tumors with the pan T cell marker CD3 to identify if our

combination therapy resulted in an increase in T cell infiltration into tumors. We observed that the increase in splenic $CD4^+$ and $CD8^+$ T lymphocytes did not reflect a general increase in T cells within tumors from either single agent or the combination of MEK162 and buparlisib (Supplementary Fig. 5C and 5D). Together, these data supported that the anti-tumor activity of MEK162 and buparlisib does not result from improved T cell-mediated immunity.

To test our second hypothetical mechanism for the anti-tumor effectiveness of our combination therapy, we examined the anti-tumor activity of MEK162 and buparlisib on the tumor cells themselves. *In vitro* studies confirmed that tumor cells were the most sensitive to the combination MEK162 and buparlisib (Fig. 6A). When tested *in vivo*, we observed that combining MEK and PI3K/Akt inhibition was efficacious at reducing the percentage of proliferating tumor cells, as assayed by Ki67 immunostaining (Fig. 6B and 6C). Tumor cell death also increased, as the percentage of cells positive for cleaved caspase-3 staining increased following dual treatment with MEK162 and buparlisib (Fig. 6B and 6D). Together, these data strongly suggest that the anti-tumor effect of combining MEK162 with buparlisib occurs through activities intrinsic to the tumor cell.

Discussion

Cachexia is perhaps the most notable side effect of advanced cancer, and no pharmacological agents are currently approved to treat this syndrome. A clinical trial in patients with advanced biliary tract cancer suggested that inhibition of MEK signaling might be an effective means to prevent cancer-induced muscle wasting (10, 11). The pre-clinical data presented here support these findings in patients and both further expand on a role for ERK activity in muscle as a regulator of cancer cachexia and identify PI3K/Akt as a complimentary pathway that can be targeted to concurrently elicit anti-tumor efficacy.

MEK inhibition as an attractive anti-cachexia therapy

Successful treatment of cancer cachexia will require both anti-tumor efficacy and protection against tumor-induced muscle wasting. Indeed, one of the long-term challenges of developing and implementing anti-cachexia therapy has been the concern that such therapies can have an unintended effect in promoting tumor growth. Many theoretical strategies of promoting muscle growth, such as stimulating protein synthesis via the PI3K/Akt pathway, have not been viewed as viable options for the treatment of cancer cachexia patients, since these same pathways are often drivers of tumor progression. We propose that inhibiting MEK is an attractive treatment option for cancer cachexia, given its low risk of promoting tumor growth and its effectiveness in preserving lean mass and total body weight in both mice and patients. Our data are consistent with two previous studies that have demonstrated an ability MEK inhibition to prevent muscle wasting induced by cancer (25, 37). In both of these studies, MEK inhibition either led to a decrease in tumor volume or an increase in body or muscle weight of non-tumor-bearing mice, making it difficult to separate the ability of MEK inhibition to prevent cancer cachexia from either direct tumor or muscle effects. In sharp contrast, our data utilizing our tumor cell line resistant to MEK162 demonstrate that MEK162 can directly prevent cancer cachexia without affecting tumor growth and without

simply promoting muscle anabolism. This is a significant advance over a number of other interventions that have reduced cachexia in animal models but not convincingly demonstrated that their anti-cachexia activity was not mediated solely by direct anti-tumor effects (27, 38-40). Further, the fact that the effectiveness of MEK162 appears to be mediated at least in part through a direct effect on skeletal muscle gives this therapy an added advantage over other potential therapies. Many therapies such as monoclonal antibodies target a single potential driver of cachexia, yet at the present time, no single cause of cachexia has been identified in cancer patients. MEK inhibition may be a better choice, as it could prevent cachexia induced by a number of factors as opposed to targeting one specific soluble factor.

MEK inhibition as a component of combinatorial therapy

While MEK inhibitors can elicit anti-tumor activity, objective responses to these agents are not frequently observed in solid tumors when administered as a monotherapy (11, 41-46). Overall, single agent MEK inhibitors have been limited as a front-line targeted therapy due to compensatory activation of other oncogenic signaling pathways (42, 47-50). This has necessitated an approach whereby MEK inhibitors are being tested in combination with other agents (51-56). Amongst the most common partners for MEK therapy are inhibitors of the PI3K/Akt pathway (50, 57-59).

Combinatorial therapy is particularly pertinent in the context of cachexia, which will be most effectively treated by both targeting the tumor and preserving skeletal muscle. We tested two hypotheses about how MEK162 and buparlisib concurrently target cachexia and tumor progression. Cell depletion experiments indicated that T cells were dispensable for the efficacy of combined therapy with MEK162 and buparlisib, suggesting that the immune modulatory effects of our combination therapy are not responsible for their anti-tumor activity. Rather, our data suggest that dual MEK and PI3K/Akt inhibition has an intrinsic impact on the tumor cells themselves by inducing cell death and limiting cell proliferation.

In our study, single agent treatment with the PI3K/Akt inhibitor buparlisib reduced the rate of tumor growth, yet body weight and muscle mass were similar to vehicle-treated tumor-bearing mice. These data are consistent with results that showed that inhibiting PI3K/Akt signaling has a negative impact on skeletal muscle (32, 33). Our data clearly demonstrate that MEK162 in combination with buparlisib targets C-26 tumor growth more effectively than either agent alone, while its ability to preserve body weight and skeletal muscle was dominant. Thus, MEK inhibition might be an ideal candidate when considering combinatorial therapy with agents that might negatively impact skeletal muscle, such as PI3K/Akt inhibition.

Taken together, our results demonstrate that MEK inhibition appears to provide a unique opportunity to protect skeletal muscle in cachexia. Patients most likely to benefit from this aspect of combined therapy involving MEK inhibitors are those with gastrointestinal cancers, which tend to be associated with cachexia and are often resistant to single agent therapies. Additionally, we envision that single agent MEK inhibition could improve patient performance status in palliative care situations. Collectively, these data inform the

mechanism behind novel applications of agents targeting the MEK pathway for clinical practice.

Supplementary Material

Refer to Web version on PubMed Central for supplementary material.

Acknowledgments

We acknowledge Dr. Patrice Lee (Array Biopharma, Inc.) for input on experiments involving MEK162. We acknowledge the OSU CCC Analytical Cytometry and Biostatistics Shared Resources for assistance with these studies. Additionally, we thank the OSU Pathology Core Facility and the OSU Solid Tumor Biology Histology Core and in particular Raleigh Kladney for assistance with immunohistochemistry.

Financial Support: Funding for this work was provided by the William Hall Fund for Liver and Pancreatic Cancer Research (T. Bekaii-Saab, G.B. Lesinski); The Division of Medical Oncology, Array Biopharma, Inc. (G.B. Lesinski); a Weiss Postdoctoral Fellowship (E.E. Talbert); an American Cancer Society Postdoctoral Fellowship, PF-15-156-01-CSM (E.E. Talbert); and The National Institutes of Health T32CA106196 (E.E. Talbert), T32CA090223 (M.R. Farren), and R01 CA180057 (D.C. Guttridge). This work was also supported by the Ohio State University Comprehensive Cancer Center Pelotonia Fellowship Program (Z. Che, M.R. Farren). Any opinions, findings and conclusions expressed in this material are those of the authors and do not necessarily reflect those of the Pelotonia Fellowship Program.

References

1. Samatar AA, Poulikakos PI. Targeting RAS-ERK signalling in cancer: promises and challenges. Nature reviews Drug discovery. Dec.2014 13:928–42. [PubMed: 25435214]
2. Ostrand-Rosenberg S, Sinha P, Chornoguz O, Ecker C. Regulating the suppressors: apoptosis and inflammation govern the survival of tumor-induced myeloid-derived suppressor cells (MDSC). Cancer immunology, immunotherapy : CII. Aug.2012 61:1319–25. [PubMed: 22546994]
3. McCubrey JA, Steelman LS, Chappell WH, Abrams SL, Wong EW, Chang F, et al. Roles of the Raf/MEK/ERK pathway in cell growth, malignant transformation and drug resistance. Biochim Biophys Acta. Aug.2007 1773:1263–84. [PubMed: 17126425]
4. Sumimoto H, Imabayashi F, Iwata T, Kawakami Y. The BRAF-MAPK signaling pathway is essential for cancer-immune evasion in human melanoma cells. J Exp Med. Jul 10.2006 203:1651–6. [PubMed: 16801397]
5. Phan VT, Wu X, Cheng JH, Sheng RX, Chung AS, Zhuang G, et al. Oncogenic RAS pathway activation promotes resistance to anti-VEGF therapy through G-CSF-induced neutrophil recruitment. Proc Natl Acad Sci U S A. Apr 9.2013 110:6079–84. [PubMed: 23530240]
6. Argiles JM, Busquets S, Toledo M, Lopez-Soriano FJ. The role of cytokines in cancer cachexia. Current opinion in supportive and palliative care. Dec.2009 3:263–8. [PubMed: 19713854]
7. Fearon K, Strasser F, Anker SD, Bosaeus I, Bruera E, Fainsinger RL, et al. Definition and classification of cancer cachexia: an international consensus. The Lancet Oncology. May.2011 12:489–95. [PubMed: 21296615]
8. Tisdale MJ. Mechanisms of cancer cachexia. Physiol Rev. Apr.2009 89:381–410. [PubMed: 19342610]
9. Stewart GD, Skipworth RJ, Fearon KC. Cancer cachexia and fatigue. Clinical medicine. Mar-Apr; 2006 6:140–3. [PubMed: 16688969]
10. Prado CM, Bekaii-Saab T, Doyle LA, Shrestha S, Ghosh S, Baracos VE, et al. Skeletal muscle anabolism is a side effect of therapy with the MEK inhibitor: selumetinib in patients with cholangiocarcinoma. Br J Cancer. May 8.2012 106:1583–6. [PubMed: 22510747]
11. Bekaii-Saab T, Phelps MA, Li X, Saji M, Goff L, Kauh JS, et al. Multi-institutional phase II study of selumetinib in patients with metastatic biliary cancers. J Clin Oncol. Jun 10.2011 29:2357–63. [PubMed: 21519026]

12. Acharyya S, Ladner KJ, Nelsen LL, Damrauer J, Reiser PJ, Swoap S, et al. Cancer cachexia is regulated by selective targeting of skeletal muscle gene products. J Clin Invest. Aug.2004 114:370–8. [PubMed: 15286803]
13. Acharyya S, Butchbach ME, Sahenk Z, Wang H, Saji M, Carathers M, et al. Dystrophin glycoprotein complex dysfunction: a regulatory link between muscular dystrophy and cancer cachexia. Cancer Cell. Nov.2005 8:421–32. [PubMed: 16286249]
14. Roberts PJ, Usary JE, Darr DB, Dillon PM, Pfefferle AD, Whittle MC, et al. Combined PI3K/mTOR and MEK inhibition provides broad antitumor activity in faithful murine cancer models. Clin Cancer Res. Oct 1.2012 18:5290–303. [PubMed: 22872574]
15. Ullman-Cullere MH, Foltz CJ. Body condition scoring: a rapid and accurate method for assessing health status in mice. Laboratory animal science. Jun.1999 49:319–23. [PubMed: 10403450]
16. He WA, Berardi E, Cardillo VM, Acharyya S, Aulino P, Thomas-Ahner J, et al. NF-kappaB-mediated Pax7 dysregulation in the muscle microenvironment promotes cancer cachexia. J Clin Invest. Oct 1.2013
17. Ascierto PA, Schadendorf D, Berking C, Agarwala SS, van Herpen CM, Queirolo P, et al. MEK162 for patients with advanced melanoma harbouring NRAS or Val600 BRAF mutations: a non-randomised, open-label phase 2 study. The Lancet Oncology. Mar.2013 14:249–56. [PubMed: 23414587]
18. Bendell JC, Rodon J, Burris HA, de Jonge M, Verweij J, Birle D, et al. Phase I, dose-escalation study of BKM120, an oral pan-Class I PI3K inhibitor, in patients with advanced solid tumors. J Clin Oncol. Jan 20.2012 30:282–90.
19. Yao W, Yue P, Zhang G, Owonikoko TK, Khuri FR, Sun SY. Enhancing therapeutic efficacy of the MEK inhibitor, MEK162, by blocking autophagy or inhibiting PI3K/Akt signaling in human lung cancer cells. Cancer Lett. Aug 1.2015 364:70–8. [PubMed: 25937299]
20. Burger MT, Pecchi S, Wagman A, Ni ZJ, Knapp M, Hendrickson T, et al. Identification of NVP-BKM120 as a Potent, Selective, Orally Bioavailable Class I PI3 Kinase Inhibitor for Treating Cancer. ACS medicinal chemistry letters. Oct 13.2011 2:774–9. [PubMed: 24900266]
21. Yang J, Bill MA, Young GS, La Perle K, Landesman Y, Shacham S, et al. Novel small molecule XPO1/CRM1 inhibitors induce nuclear accumulation of TP53, phosphorylated MAPK and apoptosis in human melanoma cells. PLoS One. 2014; 9:e102983. [PubMed: 25057921]
22. Guenterberg KD, Lesinski GB, Mundy-Bosse BL, Karpa VI, Jaime-Ramirez AC, Wei L, et al. Enhanced anti-tumor activity of interferon-alpha in SOCS1-deficient mice is mediated by CD4(+) and CD8(+) T cells. Cancer immunology, immunotherapy : CII. Sep.2011 60:1281–8. [PubMed: 21604070]
23. Kenward MG, Roger JH. Small sample inference for fixed effects from restricted maximum likelihood. Biometrics. Sep.1997 53:983–97. [PubMed: 9333350]
24. Talbert EE, Metzger GA, He WA, Guttridge DC. Modeling human cancer cachexia in colon 26 tumor-bearing adult mice. J Cachexia Sarcopenia Muscle. Dec.2014 5:321–8. [PubMed: 24668658]
25. Chacon-Cabrera A, Fermoselle C, Urtreger AJ, Mateu-Jimenez M, Diament MJ, de Kier Joffe ED, et al. Pharmacological strategies in lung cancer-induced cachexia: effects on muscle proteolysis, autophagy, structure, and weakness. J Cell Physiol. Nov.2014 229:1660–72. [PubMed: 24615622]
26. Busquets S, Toledo M, Orpí M, Massa D, Porta M, Capdevila E, et al. Myostatin blockage using actRIIB antagonism in mice bearing the Lewis lung carcinoma results in the improvement of muscle wasting and physical performance. Journal of cachexia, sarcopenia and muscle. 2012; 3:37–43.
27. Johnston AJ, Murphy KT, Jenkinson L, Laine D, Emmrich K, Faou P, et al. Targeting of Fn14 Prevents Cancer-Induced Cachexia and Prolongs Survival. Cell. Sep 10.2015 162:1365–78. [PubMed: 26359988]
28. Fujita J, Tsujinaka T, Yano M, Ebisui C, Saito H, Katsume A, et al. Anti-interleukin-6 receptor antibody prevents muscle atrophy in colon-26 adenocarcinoma-bearing mice with modulation of lysosomal and ATP-ubiquitin-dependent proteolytic pathways. International journal of cancer Journal international du cancer. 1996; 68:637–43. [PubMed: 8938147]

29. Enomoto A, Rho MC, Fukami A, Hiraku O, Komiyama K, Hayashi M. Suppression of cancer cachexia by 20S,21-epoxy-resibufogenin-3-acetate-a novel nonpeptide IL-6 receptor antagonist. Biochem Biophys Res Commun. Oct 22.2004 323:1096–102. [PubMed: 15381112]
30. Strassmann G, Fong M, Kenney JS, Jacob CO. Evidence for the involvement of interleukin 6 in experimental cancer cachexia. J Clin Invest. May.1992 89:1681–4. [PubMed: 1569207]
31. Mizushima N, Yoshimori T. How to interpret LC3 immunoblotting. Autophagy. Nov-Dec;2007 3:542–5. 2007. [PubMed: 17611390]
32. Bodine SC, Stitt TN, Gonzalez M, Kline WO, Stover GL, Bauerlein R, et al. Akt/mTOR pathway is a crucial regulator of skeletal muscle hypertrophy and can prevent muscle atrophy in vivo. Nat Cell Biol. Nov.2001 3:1014–9. [PubMed: 11715023]
33. Peng XD, Xu PZ, Chen ML, Hahn-Windgassen A, Skeen J, Jacobs J, et al. Dwarfism, impaired skin development, skeletal muscle atrophy, delayed bone development, and impeded adipogenesis in mice lacking Akt1 and Akt2. Genes Dev. Jun 1.2003 17:1352–65. [PubMed: 12782654]
34. Taniguchi K, Karin M. IL-6 and related cytokines as the critical lynchpins between inflammation and cancer. Seminars in immunology. Feb.2014 26:54–74. [PubMed: 24552665]
35. Lechner MG, Liebertz DJ, Epstein AL. Characterization of cytokine-induced myeloid-derived suppressor cells from normal human peripheral blood mononuclear cells. Journal of immunology. Aug 15.2010 185:2273–84.
36. Sinha P, Okoro C, Foell D, Freeze HH, Ostrand-Rosenberg S, Srikrishna G. Proinflammatory S100 proteins regulate the accumulation of myeloid-derived suppressor cells. Journal of immunology. Oct 1.2008 181:4666–75.
37. Penna F, Costamagna D, Fanzani A, Bonelli G, Baccino F, Costelli P. Muscle wasting and impaired myogenesis in tumor bearing mice are prevented by ERK inhibition. PloS one. 2010:5.
38. Tseng YC, Kulp SK, Lai IL, Hsu EC, He WA, Frankhouser DE, et al. Preclinical Investigation of the Novel Histone Deacetylase Inhibitor AR-42 in the Treatment of Cancer-Induced Cachexia. J Natl Cancer Inst. Dec.2015 107:djv274. [PubMed: 26464423]
39. Kir S, White JP, Kleiner S, Kazak L, Cohen P, Baracos VE, et al. Tumour-derived PTH-related protein triggers adipose tissue browning and cancer cachexia. Nature. Sep 4.2014 513:100–4. [PubMed: 25043053]
40. Kir S, Komaba H, Garcia AP, Economopoulos KP, Liu W, Lanske B, et al. PTH/PTHrP Receptor Mediates Cachexia in Models of Kidney Failure and Cancer. Cell Metab. Feb 9.2016 23:315–23. [PubMed: 26669699]
41. Carvajal RD, Sosman JA, Quevedo JF, Milhem MM, Joshua AM, Kudchadkar RR, et al. Effect of selumetinib vs chemotherapy on progression-free survival in uveal melanoma: a randomized clinical trial. JAMA. Jun 18.2014 311:2397–405. [PubMed: 24938562]
42. O'Neil BH, Goff LW, Kauh JS, Strosberg JR, Bekaii-Saab TS, Lee RM, et al. Phase II study of the mitogen-activated protein kinase 1/2 inhibitor selumetinib in patients with advanced hepatocellular carcinoma. J Clin Oncol. Jun 10.2011 29:2350–6. [PubMed: 21519015]
43. Leijen S, Middleton MR, Tresca P, Kraeber-Bodere F, Dieras V, Scheulen ME, et al. Phase I dose-escalation study of the safety, pharmacokinetics, and pharmacodynamics of the MEK inhibitor RO4987655 (CH4987655) in patients with advanced solid tumors. Clin Cancer Res. Sep 1.2012 18:4794–805. [PubMed: 22767668]
44. Infante JR, Fecher LA, Falchook GS, Nallapareddy S, Gordon MS, Becerra C, et al. Safety, pharmacokinetic, pharmacodynamic, and efficacy data for the oral MEK inhibitor trametinib: a phase 1 dose-escalation trial. The Lancet Oncology. Aug.2012 13:773–81. [PubMed: 22805291]
45. Falchook GS, Lewis KD, Infante JR, Gordon MS, Vogelzang NJ, DeMarini DJ, et al. Activity of the oral MEK inhibitor trametinib in patients with advanced melanoma: a phase 1 dose-escalation trial. The Lancet Oncology. Aug.2012 13:782–9. [PubMed: 22805292]
46. Adjei AA, Cohen RB, Franklin W, Morris C, Wilson D, Molina JR, et al. Phase I pharmacokinetic and pharmacodynamic study of the oral, small-molecule mitogen-activated protein kinase kinase 1/2 inhibitor AZD6244 (ARRY-142886) in patients with advanced cancers. J Clin Oncol. May 1.2008 26:2139–46. [PubMed: 18390968]
47. Miller CR, Oliver KE, Farley JH. MEK1/2 inhibitors in the treatment of gynecologic malignancies. Gynecologic oncology. Apr.2014 133:128–37. [PubMed: 24434059]

48. Jain N, Curran E, Iyengar NM, Diaz-Flores E, Kunnavakkam R, Popplewell L, et al. Phase II study of the oral MEK inhibitor selumetinib in advanced acute myelogenous leukemia: a University of Chicago phase II consortium trial. Clin Cancer Res. Jan 15.2014 20:490–8. [PubMed: 24178622]

49. Shen CT, Qiu ZL, Luo QY. Efficacy and safety of selumetinib compared with current therapies for advanced cancer: a meta-analysis. Asian Pacific journal of cancer prevention : APJCP. 2014; 15:2369–74. [PubMed: 24716986]

50. Kandil E, Tsumagari K, Ma J, Abd Elmageed ZY, Li X, Slakey D, et al. Synergistic inhibition of thyroid cancer by suppressing MAPK/PI3K/AKT pathways. The Journal of surgical research. Oct. 2013 184:898–906. [PubMed: 23602735]

51. Koh YW, Shah MH, Agarwal K, McCarty SK, Koo BS, Brendel VJ, et al. Sorafenib and Mek inhibition is synergistic in medullary thyroid carcinoma in vitro. Endocrine-related cancer. Feb. 2012 19:29–38. [PubMed: 22109971]

52. Gayle SS, Castellino RC, Buss MC, Nahta R. MEK inhibition increases lapatinib sensitivity via modulation of FOXM1. Current medicinal chemistry. 2013; 20:2486–99. [PubMed: 23531216]

53. Sakamoto T, Ozaki K, Fujio K, Kajikawa SH, Uesato S, Watanabe K, et al. Blockade of the ERK pathway enhances the therapeutic efficacy of the histone deacetylase inhibitor MS-275 in human tumor xenograft models. Biochem Biophys Res Commun. Apr 19.2013 433:456–62. [PubMed: 23501104]

54. Chen X, Wu Q, Tan L, Porter D, Jager MJ, Emery C, et al. Combined PKC and MEK inhibition in uveal melanoma with GNAQ and GNA11 mutations. Oncogene. Sep 25.2014 33:4724–34. [PubMed: 24141786]

55. Xu J, Knox JJ, Ibrahimov E, Chen E, Serra S, Tsao M, et al. Sequence dependence of MEK inhibitor AZD6244 combined with gemcitabine for the treatment of biliary cancer. Clin Cancer Res. Jan 1.2013 19:118–27. [PubMed: 23091117]

56. Ebert PJ, Cheung J, Yang Y, McNamara E, Hong R, Moskalenko M, et al. MAP Kinase Inhibition Promotes T Cell and Anti-tumor Activity in Combination with PD-L1 Checkpoint Blockade. Immunity. Mar 15.2016 44:609–21. [PubMed: 26944201]

57. Renshaw J, Taylor KR, Bishop R, Valenti M, De Haven Brandon A, Gowan S, et al. Dual blockade of the PI3K/AKT/mTOR (AZD8055) and RAS/MEK/ERK (AZD6244) pathways synergistically inhibits rhabdomyosarcoma cell growth in vitro and in vivo. Clin Cancer Res. Nov 1.2013 19:5940–51. [PubMed: 23918606]

58. Qu Y, Wu X, Yin Y, Yang Y, Ma D, Li H. Antitumor activity of selective MEK1/2 inhibitor AZD6244 in combination with PI3K/mTOR inhibitor BEZ235 in gefitinib-resistant NSCLC xenograft models. Journal of experimental & clinical cancer research : CR. 2014; 33:52. [PubMed: 24939055]

59. Do K, Speranza G, Bishop R, Khin S, Rubinstein L, Kinders RJ, et al. Biomarker-driven phase 2 study of MK-2206 and selumetinib (AZD6244, ARRY-142886) in patients with colorectal cancer. Investigational new drugs. Jun.2015 33:720–8. [PubMed: 25637165]

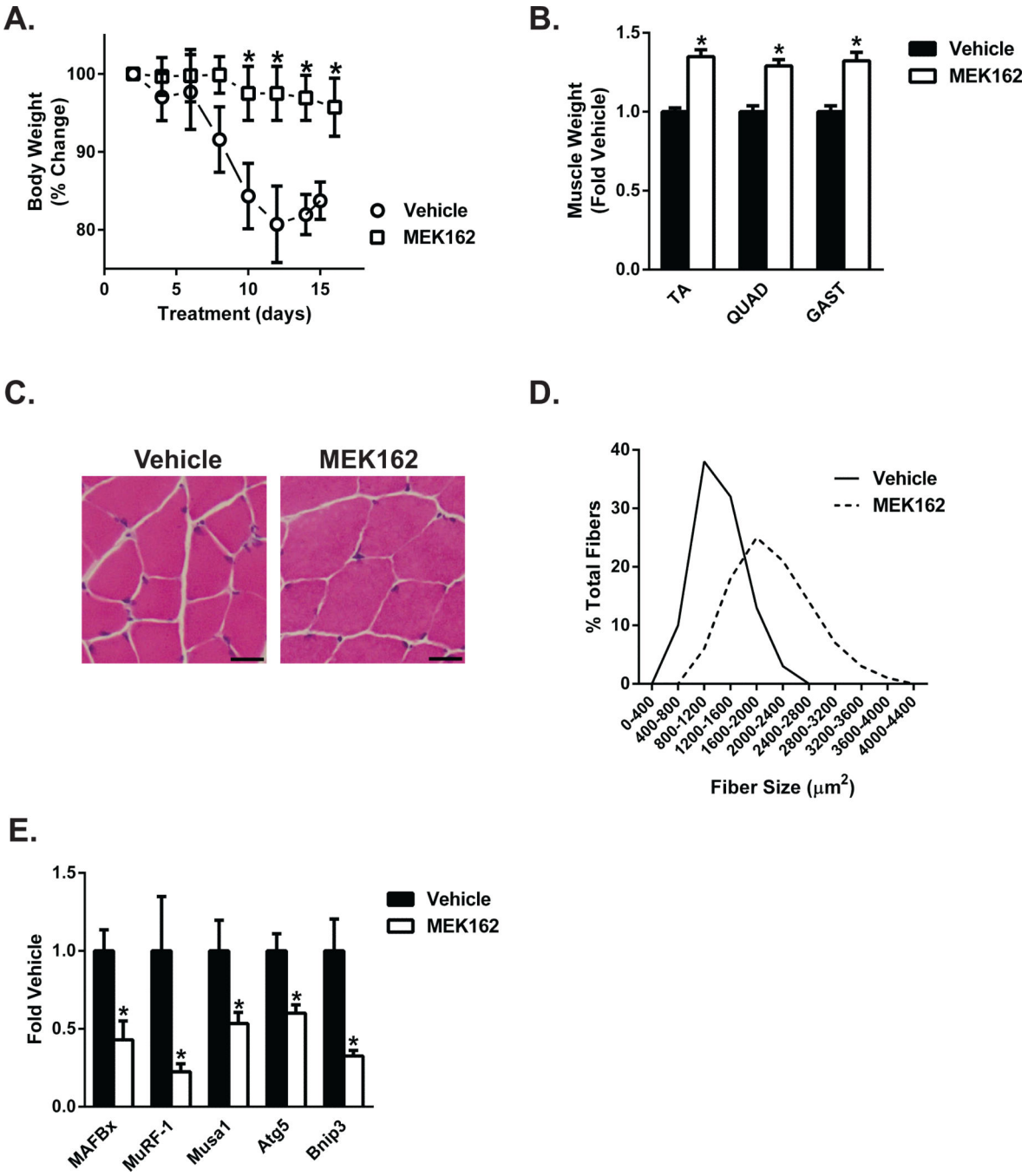

Fig 1.

MEK162 treatment prevents cancer-induced weight loss and muscle wasting. **(A)** Vehicle-treated mice progressively lost weight over the course of cancer cachexia induced by C-26 tumors, while treatment with MEK162 prevented the tumor-associated weight loss. Treatment was initiated 7 days post tumor-cell injection, to allow tumor establishment. **(B)** Treatment with MEK162 was sufficient to preserve tibialis anterior (TA), quadriceps (QUAD), and gastrocnemius (GAST) muscle masses compared to vehicle-treated mice. **(C)** Representative cross-sections demonstrating muscle fiber size from vehicle and MEK162-

treated mice bearing C-26 tumors. Scale bar = 20 μm **(D)** Treatment with MEK162 during C-26 tumor-bearing results in a right shift of GAST muscle fiber cross-sectional areas. **(E)** Treatment with MEK162 decreased expression of five muscle atrophy-associated genes in QUAD compared to vehicle-treated mice. Data are presented as mean ± standard error of the mean (SEM), n=6-7/group. * = $p<0.05$ compared to vehicle-treated mice.

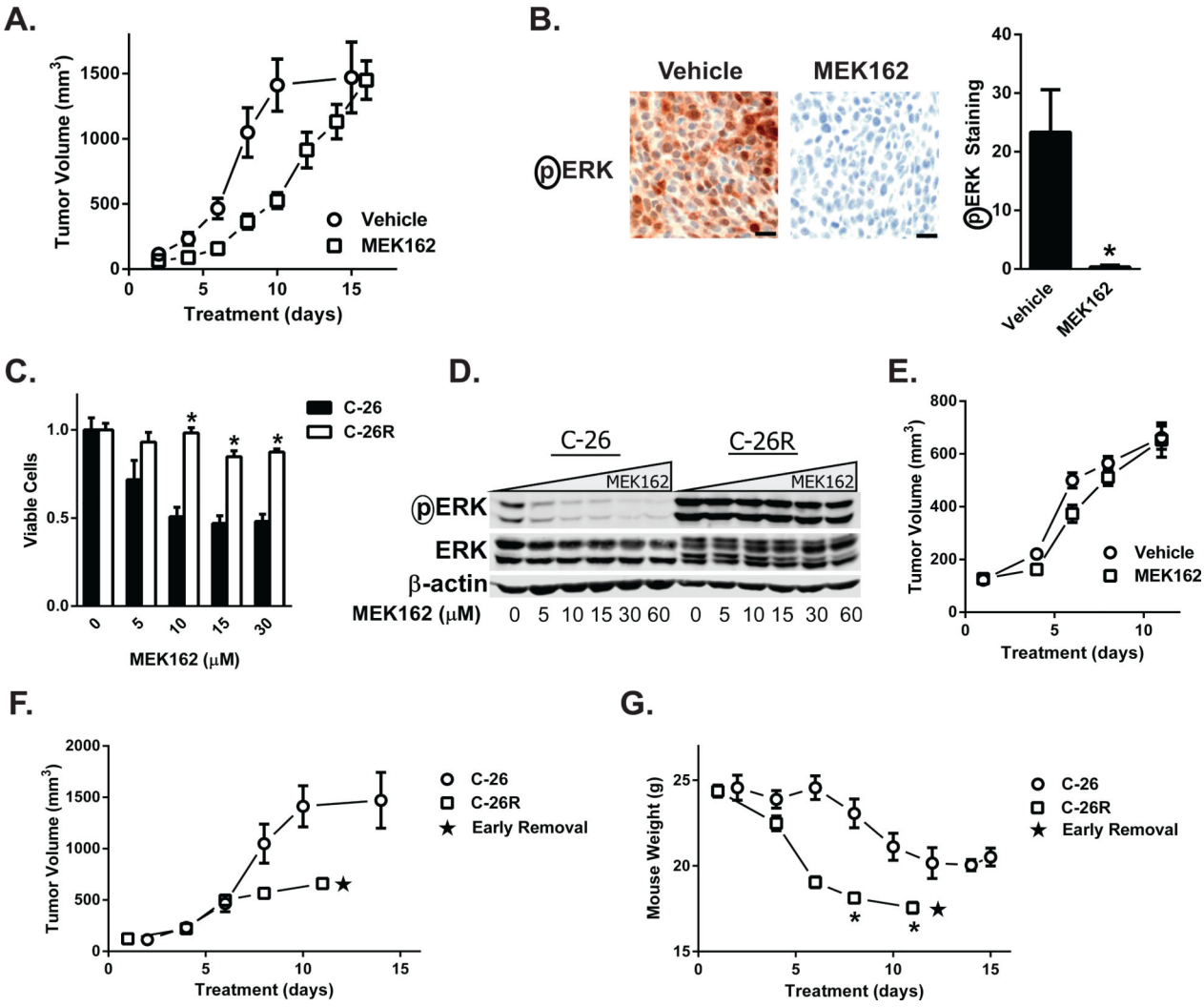

Fig. 2.

Development of a MEK162-resistant C-26 tumor cell line. **(A)** Treatment with MEK162 had a modest, but insignificant effect on the rate of tumor growth over the first 10 days of drug treatment. **(B)** Treatment of tumor-bearing mice with MEK162 decreases pERK staining in C-26 tumors. Scale bar = 20 μm **(C)** C-26 cells were made resistant to MEK162 treatment (C-26R), and maintained in culturing conditions at 30 μM. Cell viability was analyzed using a two-way ANOVA with factors of drug concentration and resistance. A significant interaction effect existed between drug concentration and resistance, with significant differences in cell survival at 10 μM, 15 μM, and 30 μM MEK162. **(D)** Treatment with MEK162 inhibits ERK phosphorylation in parental C-26 cells, but has no effect on ERK phosphorylation in C-26R cells. **(E)** Treatment of mice bearing C-26R tumors with MEK162 did not affect the rate of tumor growth. **(F)** Vehicle-treated mice bearing C-26 or C-26R tumors tend to have different rates of tumor growth (p=0.13). **(G)** Mice bearing C-26R tumors lose weight more rapidly than mice bearing parental C-26 tumors. Data are presented as mean ± standard error of the mean (SEM). *In vivo* data n=6-11/group. * = p<0.05. Panels

F and G represent tumor growth curves from vehicle-treated mice from independent experiments.

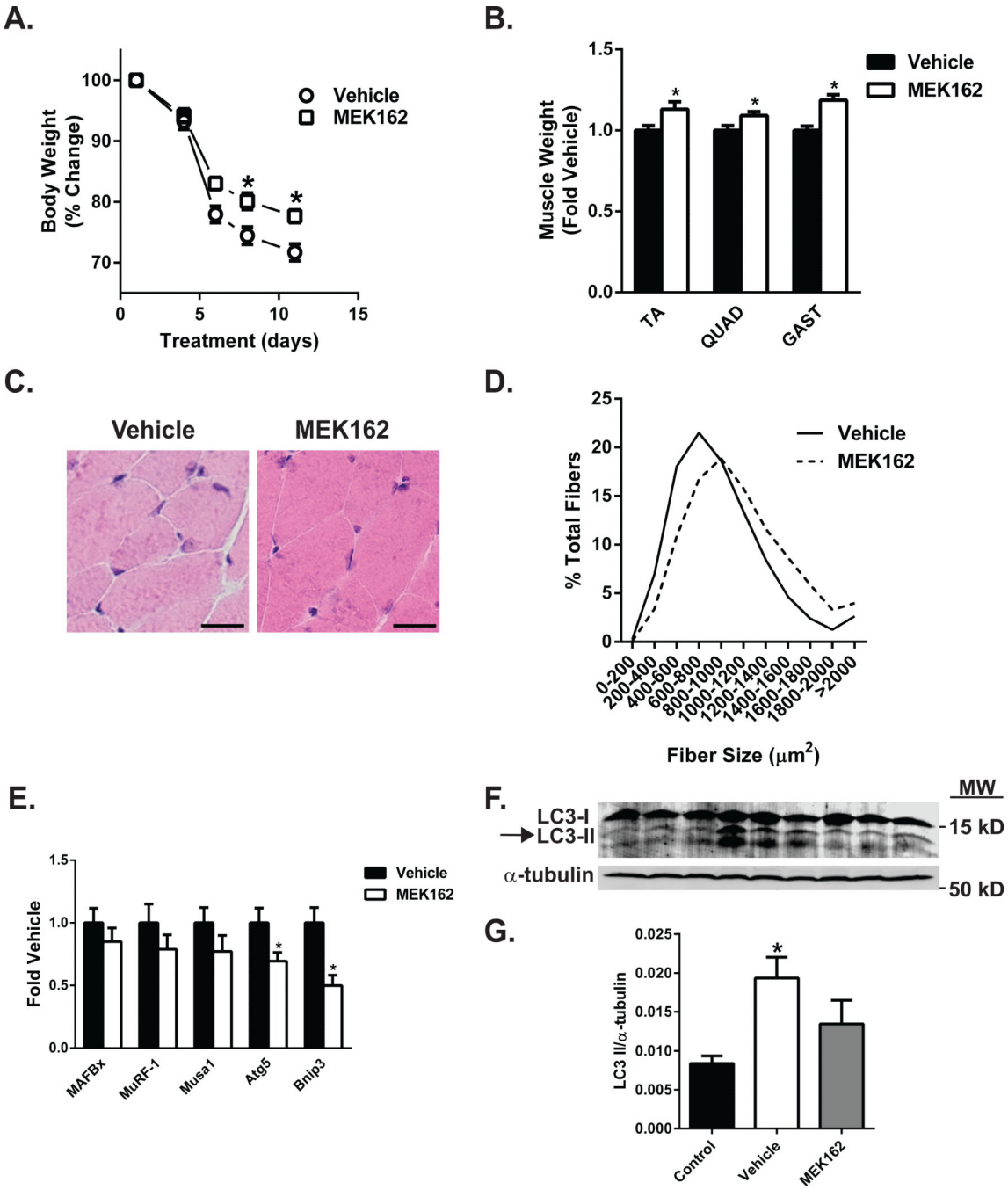

Fig 3.

MEK162 prevents cancer-induced weight loss and muscle wasting in part via a tumor extrinsic mechanism. **(A)** MEK162 treatment significantly attenuated body weight losses in mice bearing resistant C-26R tumors compared to vehicle-treated mice. **(B)** Treatment with MEK162 was sufficient to preserve tibialis anterior (TA), quadriceps (QUAD), and gastrocnemius (GAST) muscle weights compared to vehicle-treated mice. **(C)** Representative images of muscle fiber size from vehicle and MEK162-treated C-26R tumor-bearing mice. Scale bar = 20 μm **(D)** Treatment with MEK162 resulted in a right shift of

GAST muscle fiber cross-sectional areas from mice bearing C-26R tumors. **(E)** Treatment with MEK162 decreased expression of muscle atrophy-associated genes associated with autophagy in QUAD. **(F)** Autophagosome formation is increased in tumor-bearing mice, as evidenced by the increased presence of LC3-II as shown by immunoblotting (indicated by arrowhead). Treatment with MEK162 reduces LC3-II formation in tumor-bearing mice. MW designates molecular weight markers in kilodaltons. **(G)** Quantification of **(F)**. Data are presented as mean ± standard error of the mean (SEM) and represent a combination of two experiments of n=5 and n=6/group, with the exception of muscle fiber size measurements, which only include n=5/group, and the LC3 II blot, which is n=3/group. * = $p<0.05$ compared to vehicle-treated mice.

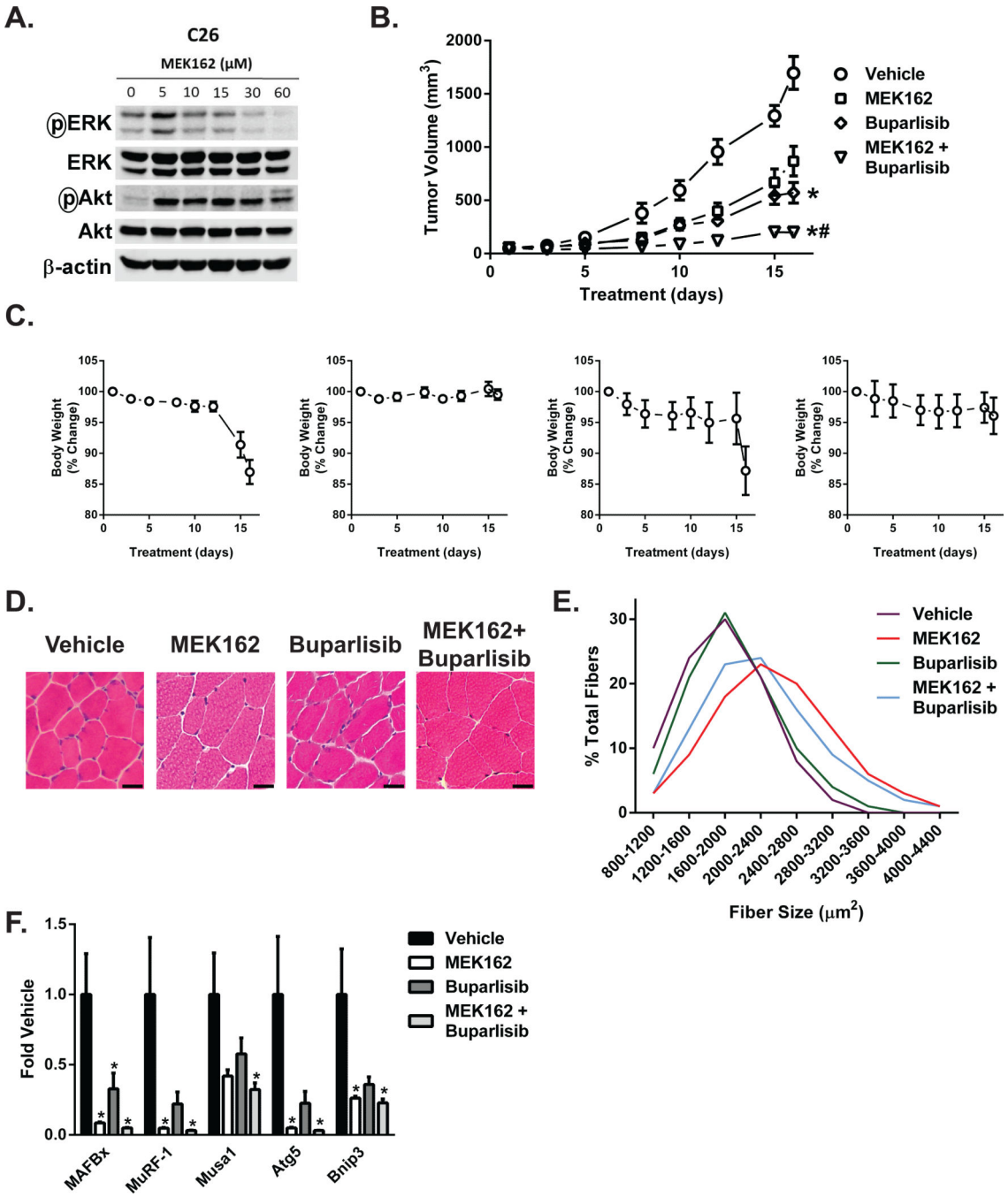

Fig 4.

MEK162 prevents cancer-induced weight loss and muscle wasting when used in combination with buparlisib. **(A)** Treatment of MEK-sensitive C-26 cells with MEK162 induced activation of the Akt pathway. **(B)** Treatment with buparlisib or MEK162 + buparlisib significantly reduced tumor growth compared to vehicle treatment. MEK162 + buparlisib further reduced tumor growth compared to MEK162 or buparlisib treatment alone. **(C)** Weight loss across the experiment. No significant differences between groups were observed across the experiment, but total weight loss is significant at the experiment

endpoint. **(D)** Representative images of muscle fiber size from vehicle and MEK162-treated mice. Scale bar = 20 μm **(E)** Treatment with MEK162 or MEK162 + buparlisib results in a right shift in the fiber size distribution of the GAST muscle compared to vehicle-treated mice. **(F)** Treatment with MEK162 + buparlisib decreased expression of five muscle atrophy-associated genes compared to vehicle-treated mice in QUAD, with MEK162 alone sufficient to decrease gene expression in four of these genes. Data are presented as mean ± standard error of the mean (SEM), n=5-6/group. * = $p<0.05$ compared to vehicle-treated mice. # = $p<0.05$ versus both single agent MEK162 and single agent buparlisib.

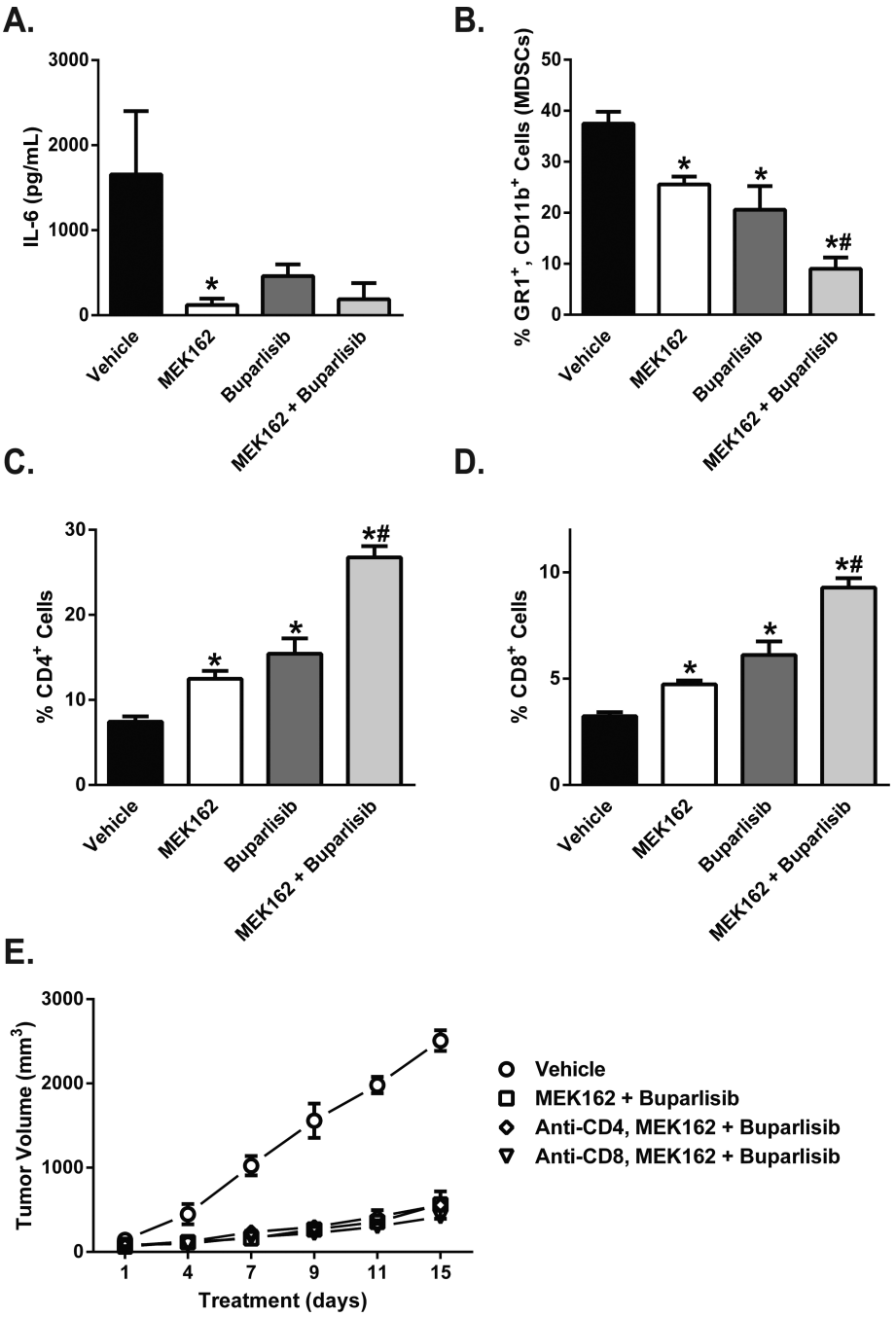

Fig 5.

MEK162 and buparlisib modulate immune biomarkers. **(A)** Treatment with MEK162 significantly reduces serum IL-6. **(B)** Treatment with either MEK162 or buparlisib is sufficient to reduce the percentage of splenic MDSCs. Combination therapy with MEK162 + buparlisib was sufficient to further reduce MDSC numbers. **(C)** Splenic $CD4^+$ T cell numbers were increased in MEK162- and buparlisib-treated mice, with further increases in MEK162 + buparlisib-treated mice. **(D)** Similar to $CD4^+$ T cell numbers, treatment with MEK162 or buparlisib significantly increased $CD8^+$ T cell numbers in tumor-bearing mice.

Treatment with MEK162 + buparlisib further increased $CD8^+$ cells compared to MEK162 or buparlisib treatment. **(E)** Depletion of $CD4^+$ or $CD8^+$ cells is not sufficient to decrease the efficacy of MEK162 + buparlisib combination therapy. Data are presented as mean ± standard error of the mean (SEM), n=5-6/group, with the exception of the depletion experiment, n=3-4/group. * = $p<0.05$ compared to vehicle-treated mice. # = $p<0.05$ versus both single agent MEK162 and single agent buparlisib.

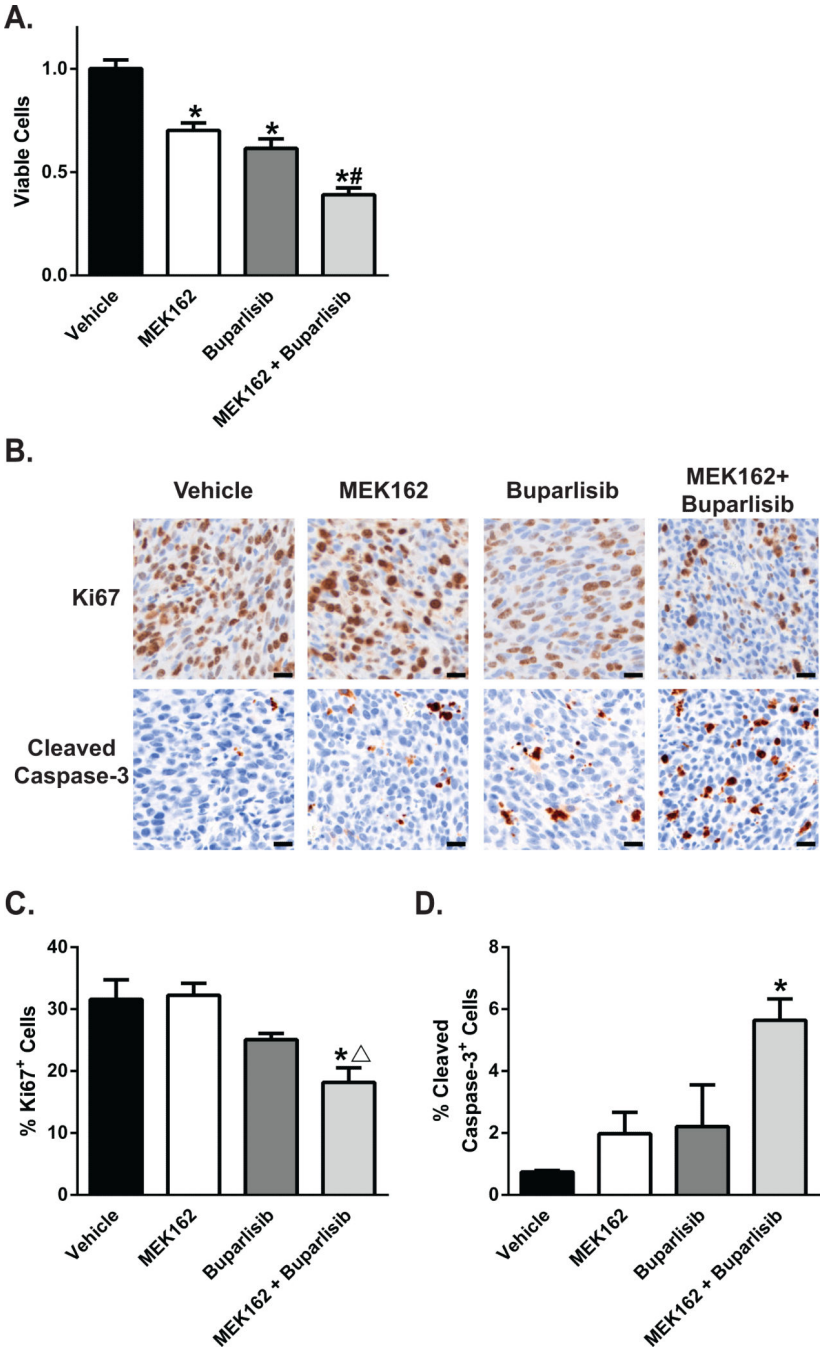

Fig 6.

MEK162 and buparlisib decrease tumor growth by a tumor cell-intrinsic mechanism. **(A)** Treatment of cultured C-26 tumor cells with MEK162 or buparlisib is sufficient to reduce cell viability, with treatment with a combination of these two agents further decreasing viability. **(B)** Representative images of tumors treated with single agent MEK162, buparlisib, or MEK162 + buparlisib for 48-72 hours stained for Ki67 or cleaved caspase-3. **(C)** Treatment with MEK162 + buparlisib for 48-72 hours decreases cell proliferation as measured by the number of Ki67-positive cells in C-26 tumors (n=3/group). **(D)** Treatment

with MEK162 + buparlisib for 48-72 hours increases the number of cleaved caspase-3-positive cells in C-26 tumors (n=3/group). * = $p<0.05$ compared to vehicle-treated mice. # = $p<0.05$ versus both single agent MEK162 and single agent buparlisib. Δ = $p<0.05$ versus single agent MEK162.